

Electronic structure of the unreconstructed 30° partial dislocation in silicon

John E. Northrup and Marvin L. Cohen

*Department of Physics, University of California, Berkeley, California 94720
and Materials and Molecular Research Division, Lawrence Berkeley Laboratory, Berkeley, California 94720*

James R. Chelikowsky

*Corporate Research Science Laboratories, Exxon Research and Engineering Company,
Linden, New Jersey 07036*

J. Spence and A. Olsen

Department of Physics, Arizona State University, Tempe, Arizona 85281

(Received 4 May 1981)

The electronic structure of the unreconstructed 30° partial dislocation in silicon is calculated using a local pseudopotential and a minimal basis set. The minimal basis set consists of *s*- and *p*-symmetry orbitals and is augmented by five *d*-symmetry orbitals. The model-core geometry is determined by high-resolution electron microscopy. The calculation indicates the existence of a one-dimensional band of dangling-bond states which propagate along the dislocation line. This band is half filled, implying metallic properties.

I. INTRODUCTION

The recent resurgence of interest in the electronic structure of dislocations in semiconductors since the early pioneering work of Shockley¹ and Read² can be traced to several factors. First, through the development of the weak-beam electron microscope technique,³ it has become clear over the past decade that the majority of dislocations in tetrahedrally coordinated semiconductors is dissociated into partial dislocations. Thus, many early conclusions² must now be reconsidered. Second, improvements in techniques for computing the electronic structure of defects and surfaces now allow large clusters of atoms to be considered, and finally, new techniques such as cathodoluminescence, temperature-dependent electron beam-induced conductivity, and scanning deep-level transient spectroscopy now offer the hope that energy levels may be measured directly from well-characterized and isolated dislocation segments. For a review of all this work, see Ref. 4.

The low-temperature deformation of Ge or Si produces predominantly dissociated screw dislocations (consisting of two 30° partials) and dissociated 60° dislocations (consisting of one 90° and one 30° partial), each with a total Burgers vector of the $(\frac{1}{2})$ [110] type and lying on the (111) slip plane. Dislocations running in other directions in the lattice are to be thought of as kinked segments of these

types. Thus, it is generally accepted⁵ that the important elemental defects (other than point defects) which control the mechanical and electronic properties of tetrahedrally coordinated semiconductors at low temperatures are the 30° partial, the 90° partial, and kinks. These dislocations may also lie on either the closely spaced (111) glide planes or on the more widely spaced (111) "shuffle" planes.⁶ Recent evidence,^{7,8} while not conclusive, favors the glide model. The shuffle and glide configurations of the 30° partial differ in the presence or absence of a single column of atoms along the dislocation core. The possibility of bond reconstruction along the core also exists, and the implications of this for electronic structure have been considered by several authors.^{9,10} Since recombination, luminescence, and lattice friction all depend on the details of core structure, the effects of reconstruction on all the partials and kinks and on the number of dangling bonds thereby created are important. The closely related problem of the dependence of dislocation velocity on doping also depends on the reconstruction schemes chosen.¹¹

Thus, there is considerable interest in the problem of determining the band structure of dislocations in order to determine the likely sites of dangling bonds and their associated deep-level recombination centers and to clarify the nature of the conductivity along the dislocation core, which includes the possibilities of donor or acceptor bands,

hopping conductivity, and a one-dimensional metal-insulator transition. Two calculations exist in the literature for the electronic structure of the 30° partial based on empirical extended-Huckel theory⁹ and on the continued-fraction Green's-function expansion method.¹⁰ These calculations are in broad agreement. Since we believe that the phase-dependent chemical orbital pseudopotential method¹² possesses certain advantages for problems of this type and because of the success of the closely related pseudopotential method in predicting the bulk properties of elemental crystals¹³ and their surfaces,¹⁴ we have recently completed the calculation reported below of the electronic structure of the unreconstructed 30° partial dislocation in silicon. The encouraging agreement found with the results of other workers leads us to believe that these preliminary calculations can now be applied with confidence to kinks and other line defects in semiconductors and eventually used to investigate the effect of impurity decoration.

II. ATOMIC MODELS

The atomic coordinates used for our calculation were taken from near-atomic resolution computed electron micrographs which were found to give a good fit with experimental near-atomic resolution electron images of an end-on dissociated 60° dislocation in silicon.⁷ By comparing computed images of the shuffle and glide cases with the experimental image, it was found that the experimental image clearly favors the glide model for the core of the 30° partial in this particular case. It cannot be

claimed, however, that these experimental high-resolution images are sufficiently well resolved to provide accurate core atom coordinates. All we have done⁷ is to distinguish between the two most probable structures for the core. The sub-angstrom details of the core charge distribution on which the electronic structure depends are not resolvable using current electron microscopes, which at best reveal structural detail down to about 2 \AA and have images depending sensitively on the electron-optical parameters and specimen thickness.

Figure 1 shows a diagrammatic sketch of the 30° partial. The experimental electron micrograph is shown in Fig. 2. The analysis and interpretation of this image has been given elsewhere.⁷ In this image, each black blob is an unresolved pair of atomic columns in the diamond structure seen end-on in the $[110]$ projection, and white areas are tunnels through the structure. Figure 3 shows the computed image which was found to give the best match for Fig. 2 if based on the glide-type 30° partial. This image was generated from a full numerical solution of the time-independent Schrödinger equation for the problem of the coherent multiple scattering of a fast (100 kV) electron by a thin foil and image synthesis by electron optics. Numerical solution of the high-energy electron scattering problem and the solution of the band structure both require a model which is periodic and which contains no unphysical bonds introduced by the periodic continuation implied by the use of Fourier series. This was achieved by introducing two 30° partial dislocations separated by a strip of stacking fault into an orthorhombic unit cell ($a_0=26.95 \text{ \AA}$, $b_0=9.41 \text{ \AA}$, $c_0=3.84 \text{ \AA}$, $\alpha=\beta=\gamma=90^\circ$) with op-

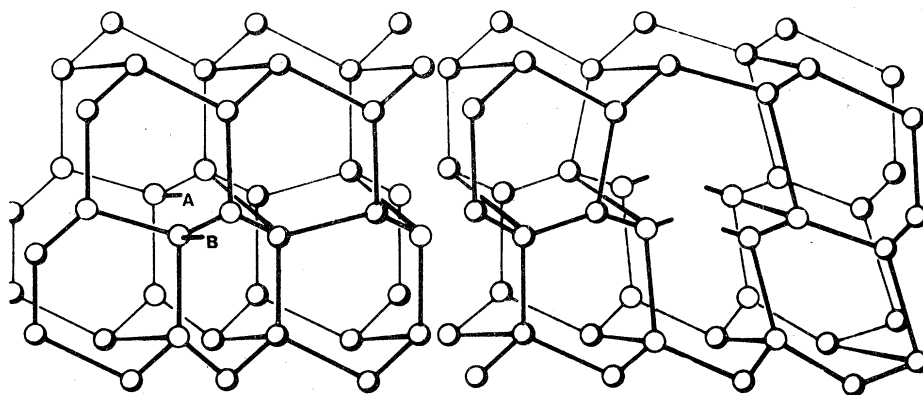


FIG. 1. Diagrammatic sketch of a 60° dislocation in silicon dissociated into an unreconstructed 30° partial on the left and a 90° partial on the right. The dislocation line runs in the $[110]$ direction and joins the dangling bonds shown at A and B. These are bonded in pairs in the 30° partial reconstruction scheme. The partials are connected by an intrinsic stacking fault of which only a portion is shown.

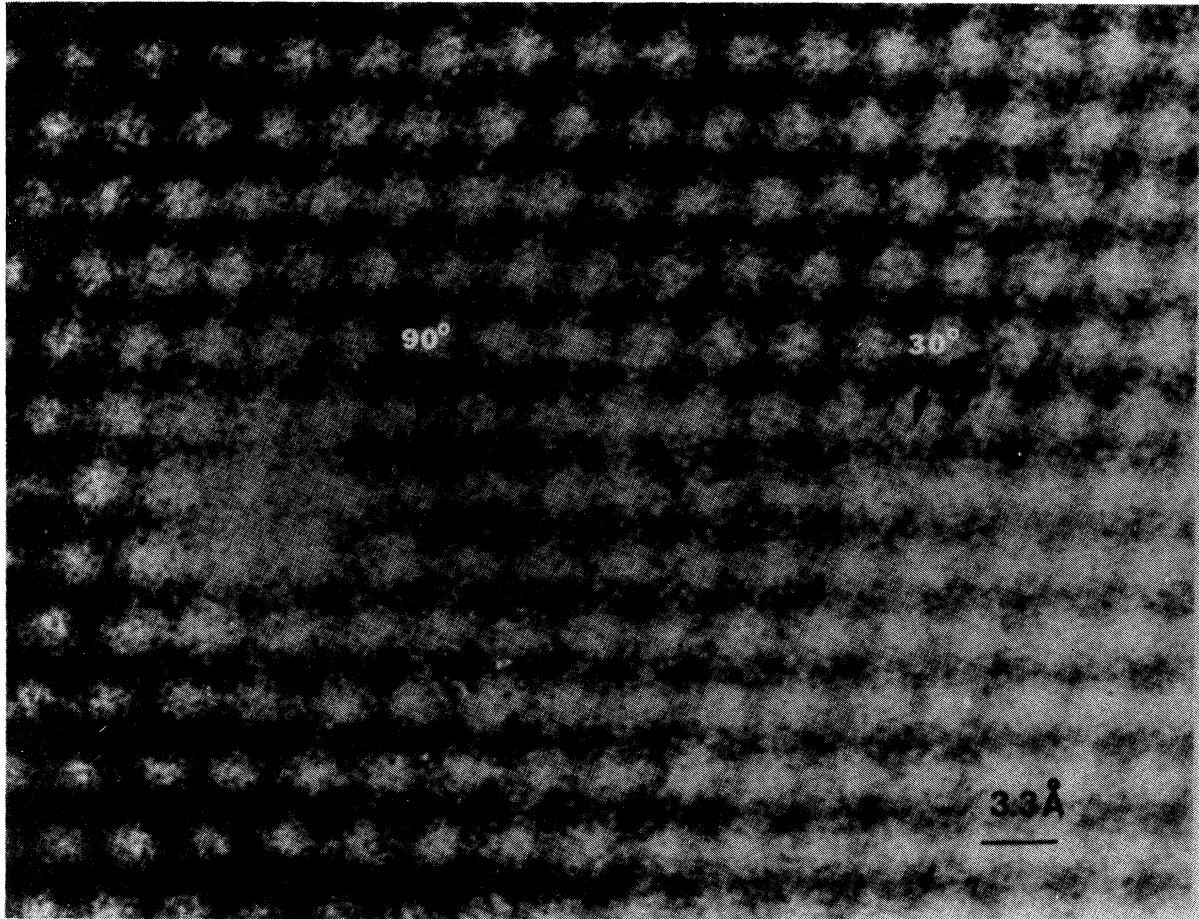


FIG. 2. Experimental high-resolution electron micrograph (lattice image) of a dissociated 60° dislocation in silicon. Each black blob in the image is an unresolved pair of atomic columns seen in the [110] projection. The crystal thickness in the projection direction is 61 Å.

posite Burgers vectors. The directions of the axes of this artificial superlattice cell are $x = [11\bar{2}]$, $y = [111]$, and $z = [1\bar{1}0]$ (the dislocation line direction) when referring to the conventional diamond cubic unit cell. This structure is three-dimensionally periodic, contains a center of symmetry, and for a sufficiently large unit cell, contains no unphysical bonds since by St. Venant's principle¹⁶ the strain is then zero at the cell boundaries. Our cell contains 48 atoms including those whose positions are related by the center of symmetry. A projection of the atomic positions onto the xy plane is shown in Fig. 4. The coordinates of the atoms are shown in Table I. The maximum bond-length distortion introduced at the cell boundary is $\sim 17\%$, which produces some gap states which are not intrinsic to the dislocation. In the real crystal, the structure (for a dissociated 60° dislocation) is periodic along

the dislocation line direction, and the stacking sequence of planes normal to this direction is $ABA-BAB$ as for the perfect crystal.

III. CALCULATIONAL PROCEDURE

The electronic structure calculations are based on the approximation that the pseudopotential may be represented in real space as a sum of atom-centered Gaussians,

$$V(\vec{r}) = \sum_{\vec{R}, \vec{\tau}_\mu} v(\vec{r} - \vec{R} - \vec{\tau}_\mu), \quad (1a)$$

$$v(r) = \sum_{i=1}^2 a_i e^{-b_i r^2}, \quad (1b)$$

where \vec{R} is a lattice vector and the a_i and b_i are determined from a nonlinear least-squares fit to a

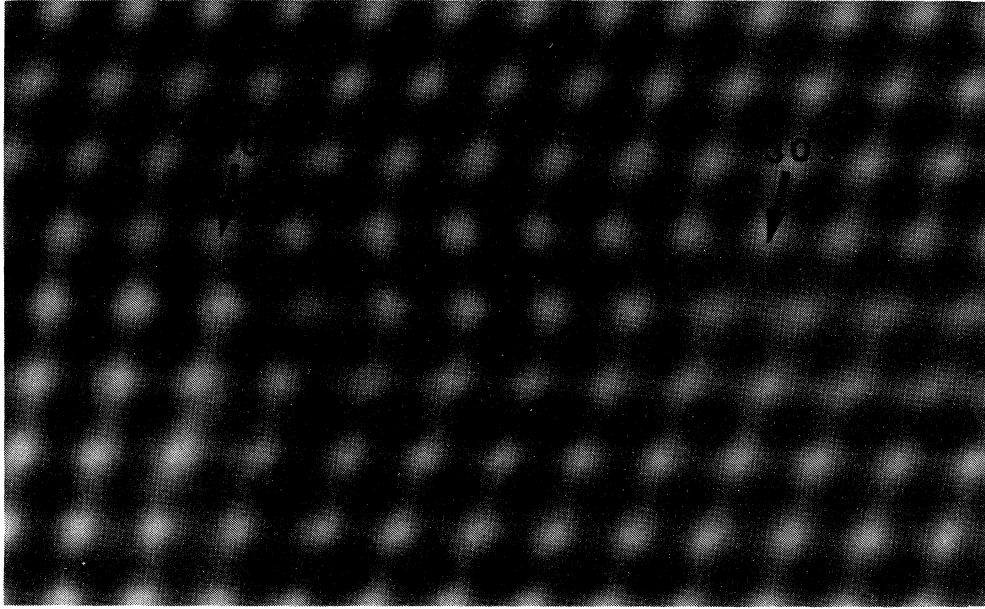


FIG. 3. Computer-simulated electron micrograph of the dislocation shown in Fig. 2. This image was computed for the dissociated glide dislocation structure by numerical solution of the Schrödinger equation using measured values of all the relevant electron-optical parameters. A point resolution limit of 3.8 Å was used as well as an "information resolution limit" of 2 Å (Ref. 15).

TABLE I. Atomic coordinates (a.u.).

Atom	x	y	z
1	25.47	-6.51	3.63
2	18.70	-6.88	0
3	12.94	-7.24	3.63
4	6.32	-7.09	0
5	0.15	-6.58	3.85
6	6.32	6.21	-0.22
7	12.63	6.19	3.63
8	18.90	6.47	0
9	20.99	5.25	3.63
10	14.47	4.78	0
11	7.85	4.86	3.63
12	1.63	5.16	-0.91
13	4.74	-5.46	4.35
14	10.70	-5.74	0
15	17.47	-5.47	3.63
16	23.03	-4.93	0
17	21.24	0.44	3.63
18	14.93	0.21	0
19	7.23	0.53	1.72
20	1.12	0.60	-1.81
21	5.04	-1.12	-2.03
22	10.85	-1.60	0.94
23	17.22	-1.05	3.63
24	23.18	-0.68	0

self-consistent crystalline pseudopotential.¹² Expressed in Ry a.u., the parameters are $a_1 = -7.744$, $a_2 = 10.362$, $b_1 = 0.38$, $b_2 = 0.76$. It is assumed that the a_i and b_i do not change for any atomic site when one passes from crystalline silicon to dislocated silicon. This assumption is tested by calculating the electronic structure of the silicon (111) surface and comparing the results with a self-consistent calculation. The energies of the surface states are found to be within ~ 0.2 eV of the self-consistent results. The lack of self-consistency is likely to induce errors of similar magnitude for the dislocation.

The basis functions are of the form

$$\phi_{\mu\nu}(\vec{k}, \vec{r}) = \sum_{\vec{R}} e^{i\vec{k} \cdot (\vec{R} + \vec{\tau}_\mu)} f_\nu(\vec{r} - \vec{R} - \vec{\tau}_\mu), \quad (2)$$

where $\vec{\tau}_\mu$ locates the atomic sites in a unit cell and ν indicates the orbital types. The f_ν are of the form

$$f_\nu(\vec{r}) = g_\nu(\vec{r}) e^{-\alpha r^2}, \quad (3)$$

where the g_ν are polynomials of s , p , and d symmetry. There are two s -like, three p -like, and five d -like functions per atom. α is set equal to 0.186, which is near the value suggested by Kane.¹⁷ With

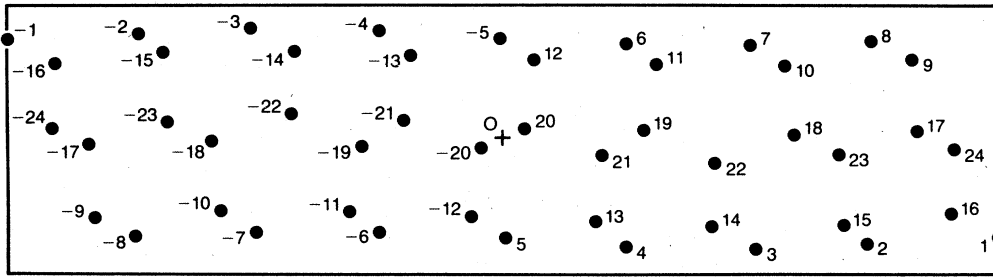


FIG. 4. A projection of the atomic positions onto the xy plane of the unit cell. Atom n is related to atom $-n$ by inversion through the origin O . Atom 22 (-22) is the dislocation core atom which terminates the extra plane (22, 14, 3) of atoms in the crystal.

this real-space representation of the potential and basis functions, we are able to calculate the Hamiltonian matrix elements for the dislocation without recourse to empirical scaling formulas.

With 10 orbitals per atom and 48 atoms per unit cell, the dimension of the Hamiltonian matrix is 480. In order to reduce the size of the matrix while still retaining some of the variational content of the d -symmetry orbitals, we employ Louie's method of phase-dependent chemical orbitals.¹² Louie has shown that by properly preparing the s , p , and d orbitals, one may treat the d orbitals in a modified form of Löwdin perturbation theory. In

this method, the variational content of the d orbitals is included implicitly in an effective Hamiltonian whose dimension is determined by the number of s and p orbitals. This procedure reduces the dimension of the matrix by a factor of 2.

IV. RESULTS

The calculations indicate the existence of a half-filled band of dangling-bond states associated with the dislocation core. The energy spectrum of the dislocation states together with the crystalline projected band structure is shown in Fig. 5. The crystalline band structure has been projected onto the

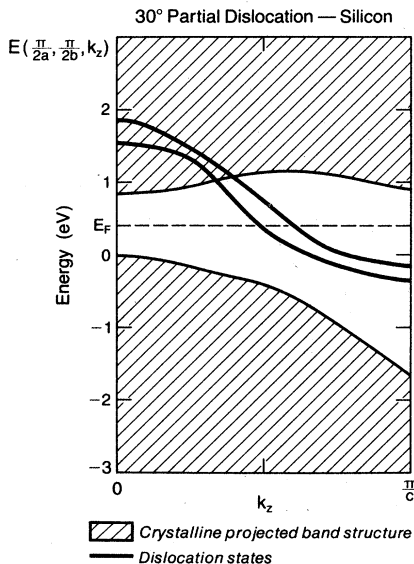


FIG. 5. Energy spectrum of the dislocation states and crystalline projected band structure. The occurrence of two dislocation bands arises from the presence of two dislocations in each unit cell. The energy splitting of these two bands is a measure of the interaction between the two dislocations. The Fermi level is indicated by the dotted line.

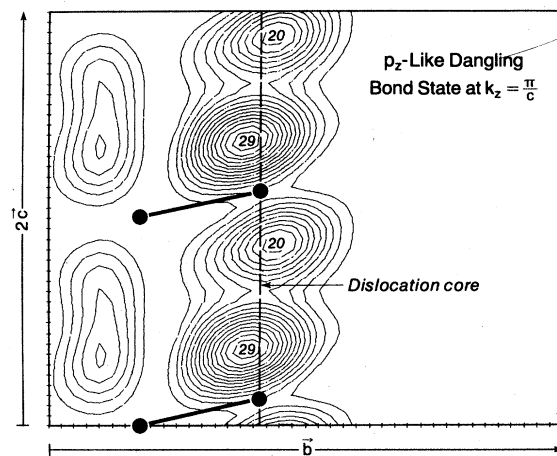


FIG. 6. Charge density of a dislocation state with $k_z = \pi/c$. The state is predominantly p_z in character and is confined to the atoms near the dislocation core which is indicated by the dotted line. One unit of charge density corresponds to e/Ω where $\Omega = 6571.7a_B^3$. The contour spacing is 2.0 units. The dislocation core line is parallel to the $[1\bar{1}0]$ direction of dislocation-free silicon. The plane shown contains atoms number 22 and 14.

Γ -to- K direction of the diamond Brillouin zone, since this is the only direction for which the translational symmetry of the crystal is not broken by the dislocation. Two dislocation bands appear in the spectrum because there are two dislocations per unit cell. The two bands are split in energy by about 0.3 eV. This splitting arises from the interaction between the two dislocations.

At $k_z=0$, the dislocation states lie in the bulk conduction-band continuum where they interact strongly with bulk conduction-band states. At this point in \vec{k} space, the dislocation-state wave functions are, therefore, not strongly localized to the core region. In the region of \vec{k} space where the dislocation states are occupied, the energies are well outside the bulk projected band structure and are, consequently, highly localized to the dislocation core.

The charge density of a dislocation state with $k_z=\pi/c$ is shown in Fig. 6. The character is predominantly p -like pointing in a direction almost parallel to the dislocation line, and the charge is strongly localized to the dislocation line. The dislocation states may, therefore, be modeled by a one-dimensional array of p_z orbitals which interact with their nearest neighbors to form a band with a dispersion relation of the form

$$E(k_z) = E_0 + 2t \cos k_z c, \quad (4)$$

where t is the nearest-neighbor hopping matrix element. Since the pseudopotential is attractive in the region between the core atoms, where the p_z orbitals have a large negative overlap, the matrix element t is greater than zero. This crude model accounts qualitatively for the dispersion shown in Fig. 5. The width of the dislocation band is ~ 1.8 eV. Marklund has obtained a p_z -like band of dangling-bond states of roughly the same width.⁹

In order to test the adequacy of the size of the

unit cell, we have calculated $E(k_x, k_y, k_z)$ for two sets of (k_x, k_y) . For a very large unit cell, the energy of a dislocation state for a given k_z will not depend on (k_x, k_y) . For a given k_z , we find the difference in energy for the dislocation states with (k_x, k_y) equal to $(0,0)$ and $(\pi/2a, \pi/2b)$ to be less than ~ 0.2 eV, which indicates that the interaction between dislocations in adjacent cells is relatively small. In addition, we find that the charge densities for the two dislocation states at $(0,0, \pi/c)$ and $(\pi/2a, \pi/2b, \pi/c)$ are essentially identical. We conclude that the unit cell is large enough to calculate successfully the properties of core-localized states.

It is generally believed that the electronic structure associated with the 30° partial dislocation in silicon consists of a full donor band and an empty acceptor band.⁵ It is, therefore, unlikely that the unreconstructed core geometry is the true geometry since it implies, if spin correlation effects are neglected, a single half-filled band. If the core undergoes a reconstruction in which the translational period along the dislocation line increases by a factor of 2, one empty and one full band separated by one energy gap will be obtained.¹⁸ Marklund has considered one reconstruction pattern for the core atoms and finds an energy gap of ~ 0.8 eV separating the filled and empty bands.

ACKNOWLEDGMENTS

We would like to thank S.G. Louie for many helpful discussions. This work was supported by the National Science Foundation Grants Nos. DMR7822465 (M.L.C.) and DAAG-29-80-0080 (J.S.) and by the Director, Office of Energy Research, Office of Basic Energy Sciences, Materials Sciences Division of the U.S. Department of Energy under Contract No. W-7405-ENG-48.

¹W. Shockley, Phys. Rev. **91**, 228 (1953).

²W. T. Read, Jr., Philos. Mag. **45**, 775 (1954).

³D. J. H. Cockayne, J. Microsc. Oxford **98**, 116 (1973).

⁴J. Phys. (Paris) Colloq. **40**, (6) (1979).

⁵P. B. Hirsch, J. Microsc. Oxford **118**, 3 (1980).

⁶J. P. Hirth and J. Lothe, *Theory of Dislocations* (McGraw-Hill, New York, 1968).

⁷A. Olsen and J. C. H. Spence, Philos. Mag. (in press).

⁸K. Wessel and H. Alexander, Philos. Mag. **35**, 1523 (1977).

⁹S. Marklund, Phys. Status Solidi B **92**, 83 (1979).

¹⁰R. Jones, J. Phys. (Paris) Colloq. **40**, (6) C6-33 (1979).

¹¹P. B. Hirsch, J. Phys. (Paris) Colloq. **40**, (6) C6-117

(1979).

¹²S. G. Louie, Phys. Rev. B **22**, 1933 (1980).

¹³M. T. Yin and M. L. Cohen, Phys. Rev. Lett. **45**, 1004 (1980).

¹⁴J. Ihm and M. L. Cohen, Phys. Rev. B **21**, 1527 (1980).

¹⁵J. C. H. Spence, *Experimental High Resolution Electron Microscopy* (Oxford University Press, Oxford, 1981).

¹⁶*Handbook of Physics*, edited by E. U. Condon and H. Odishaw (McGraw-Hill, New York, 1958), pp. 3-64.

¹⁷E. O. Kane, Phys. Rev. B **13**, 3478 (1976).

¹⁸R. E. Peierls, *Quantum Theory of Solids* (Oxford University Press, London, 1974), p. 108.

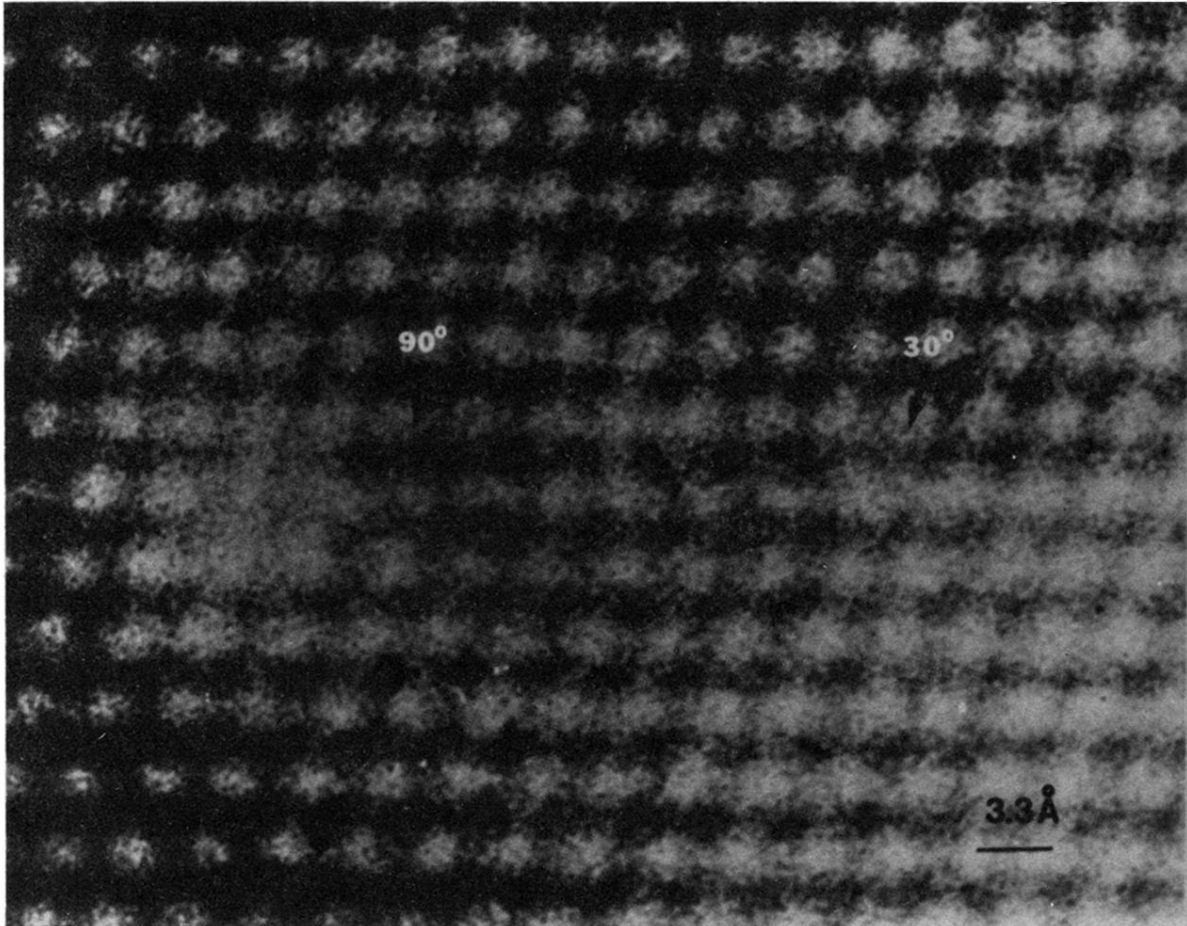


FIG. 2. Experimental high-resolution electron micrograph (lattice image) of a dissociated 60° dislocation in silicon. Each black blob in the image is an unresolved pair of atomic columns seen in the $[110]$ projection. The crystal thickness in the projection direction is 61 \AA .

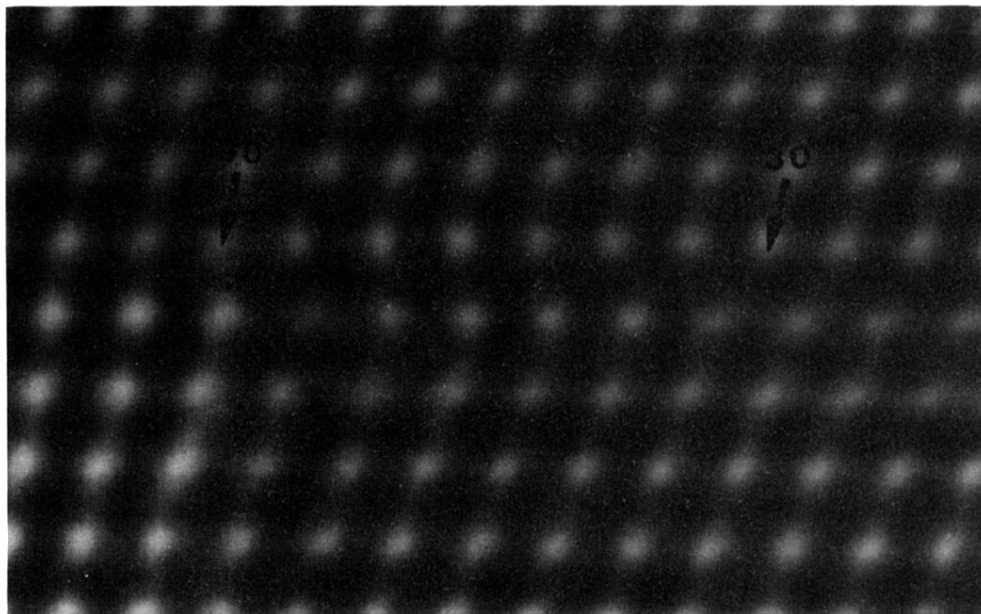


FIG. 3. Computer-simulated electron micrograph of the dislocation shown in Fig. 2. This image was computed for the dissociated glide dislocation structure by numerical solution of the Schrödinger equation using measured values of all the relevant electron-optical parameters. A point resolution limit of 3.8 \AA was used as well as an "information resolution limit" of 2 \AA (Ref. 15).